

Towards an automated OMA testing approach for modal feature extraction for wind turbine blades

J.F. Hansen¹, M.Ø.Ø. Juul², E. Orlowitz³

¹ Aarhus University, Department of Civil and Architectural Engineering,
8000 Aarhus C, Denmark

² Manobiak ApS,
8660 Skanderborg, Denmark

³ Siemens Gamesa Renewable Energy A/S,
7330 Brande, Denmark

Abstract

The aim of the work in this paper is to demonstrate the feasibility of a standardized modal test procedure for wind turbine blades that is reliable and repeatable with minimal effort. In the current approach, we excite the blade using a set of 3 inertial shakers, placed in various configurations along the length of the blade. The input forces, flat broadband, generated by the shakers are not measured. The baseline or reference test procedure is to excite the blade manually. We show that the natural frequencies extracted from the shaker tests are the same, within the bounds of uncertainty, as the natural frequencies obtained from the reference tests. The investigation is solely experimental and based on modal data collected from a test setup of a 3.4 *m* long wind turbine blade. A total of 164 modal tests were undertaken including 32 reference tests and 132 tests from 4 different shaker configurations.

1 Introduction

The task of determining the modal characteristics of a large structural component, such as a wind turbine blade, is time-consuming and can be rather challenging. The testing approaches readily available are either Experimental Modal Analysis (EMA) or Operational Modal Analysis (OMA). Traditionally, EMA has been the methodology of choice for extracting modal features of a structure. This procedure requires both measures of the input force and the corresponding structural response [1]. Whether the input is provided via shaker(s) or impact hammer, well-defined input forces are paramount to a successful modal test. Using the traditional approach on a large structure presents the obvious challenge of producing a series of well-defined force inputs, adequately exciting the structure. The need for output-only modal analysis originates from the input challenges of a large structure EMA test. In OMA we rely on the forces produced by the operating conditions to excite the structure, assuming the excitation to be randomly distributed on the structure and ideally to have white noise characteristics [2, 3]. Consequently, all modes of the system are equally excited, and closely spaced modes can be separated and identified. In reality, this assumption does not hold, however, if the modes of interest are adequately excited, i.e. present in the measured output with an acceptable SNR, the output data qualifies for modal feature extraction.

Currently, a modern wind turbine blade has a length from 80 up to 120 *m* and in the test stand the tip of the blade usually sits +15 *m* above the ground. An EMA test using the roving impact hammer approach on a specimen of that size is rather impractical and the shaker approach requires sets of suspended shakers. The appeal of OMA, in this case, is the convenience of not having to produce inputs with the same level of attention to detail as in EMA. However, OMA in an “in-laboratory” test configuration the blade excitation cannot be drawn from the surroundings and manual random excitation must be produced. It can be quite

a challenge to produce broadband randomly distributed excitation on an 80 *m* long wind turbine blade "by hand". Furthermore, due to the low natural frequency of the first mode (<1 *Hz*), the test has to be quite lengthy as well. Lastly, the repeatability of a manual OMA can be relatively poor.

The experimental investigation in this paper is motivated by the question: "How far would we be off if we just place a few shakers on the blade, input white noise, and extract the modal parameters using output-only algorithms?". By doing so we would not meet the fundamental OMA assumption of spatial input randomness. Furthermore, we add point masses to the structure. On the other hand we gain an automated, practical, and repeatable test procedure with a minimum of preparation.

2 Method

To investigate the accuracy and feasibility of the proposed approach a total of 164 modal tests on a small wind turbine blade were undertaken. The experimental test campaign featured both tests with manual excitation and tests with shaker excitation in various configurations. The duration of all modal tests complied with the OMA literature [2, 3]. The test methodology of exciting the test specimen manually posed as the reference.

The shakers were placed on the blade in 4 different configurations and the output of the shakers was (approximately) white noise, see figure 3. To keep the system mass consistent throughout all tests, shaker equivalent masses were attached to the blade in every shaker (mountable) position. The configurations 1 to 3 consisted of various groupings of the shakers; close to the root of the blade, mid-blade, and blade-tip, respectively. In configuration 4, the shakers were distributed from the root to mid-blade.

A total of 8 modes of the blade were estimated using of an output-only feature extraction algorithm. The results presented are the mean and standard deviation of the natural frequencies for the reference tests and each of the shaker tests.

2.1 Experimental setup

The test specimen of the experimental investigation was a 3.4 *m* long Olsen wind turbine blade, type OLV 340 6/10 Tip-Brake [4]. The blade was bolted/clamped to a steel mount which was sitting on, and fixed to, a cast-iron strong floor. The tip-brake steel connection rod was glued to the insertion hole with an epoxy adhesive.



(a) Olsen blade in the steel mount



(b) Sensor, shakers, masses

Figure 1: Pictures of the experimental setup

The data acquisition system consisted of four 4-channel analog input modules, type NI 9234, mounted in an 8-slot chassis, type NI cDAQ-9178. The structural response was measured through 15 uni-axial accelerometers, type B&K 4508B-002, with a sensitivity of 1 *V/g*. In the shaker tests, the input excitation was generated

using 3 miniature inertial shakers from the Modalshop, model 2002E, powered by a mini smart amplifier, model 2000. The input signals sent to the shakers were created in LabVIEW and generated by a 4-channel output module, type NI-9263. Along the length of the blade, thirteen 3D-printed shaker mounts were glued onto the blade, to enable fast and easy relocation of the shakers. As mentioned, masses were attached to the shaker mounts to eliminate the mass loading aspect of the approach. In figure 2, sensor positions and orientations, along with the layout of the shaker mounts, are shown.

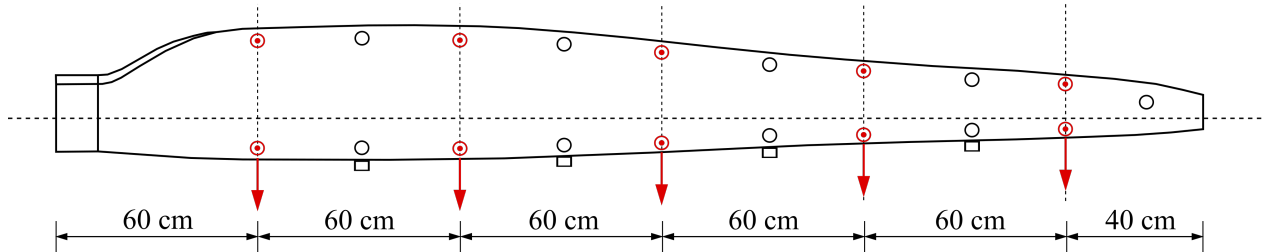


Figure 2: Schematic of the sensor and mass layout. Accelerometers: $\odot \rightarrow$, Mounts: $\circ \square$

2.2 Input force/excitation

To achieve a proper excitation of the test specimen, the miniature shakers had to produce a flat broadband force input. The optimal force performance of the shakers lies within a 20 to 3000 Hz frequency range. So, by passing a spectrally flat noise signal through the shakers, a drop-off in the lower region ($<20 Hz$) of the output frequency spectrum was to be expected. Since the initial 3 modes of the test specimen are lower than 20 Hz, the shaker input signal has to compensate for the aforementioned drop-off. Therefore, a continuous noise waveform with a frequency spectrum that was inversely proportional to frequency over a specific frequency range was used as shaker input signal. Figure 3 shows the shaker output spectra of the shakers using Gaussian white noise and inverse filter noise input, respectively. The RMS value of both shaker input signals had an RMS value of 1 V.

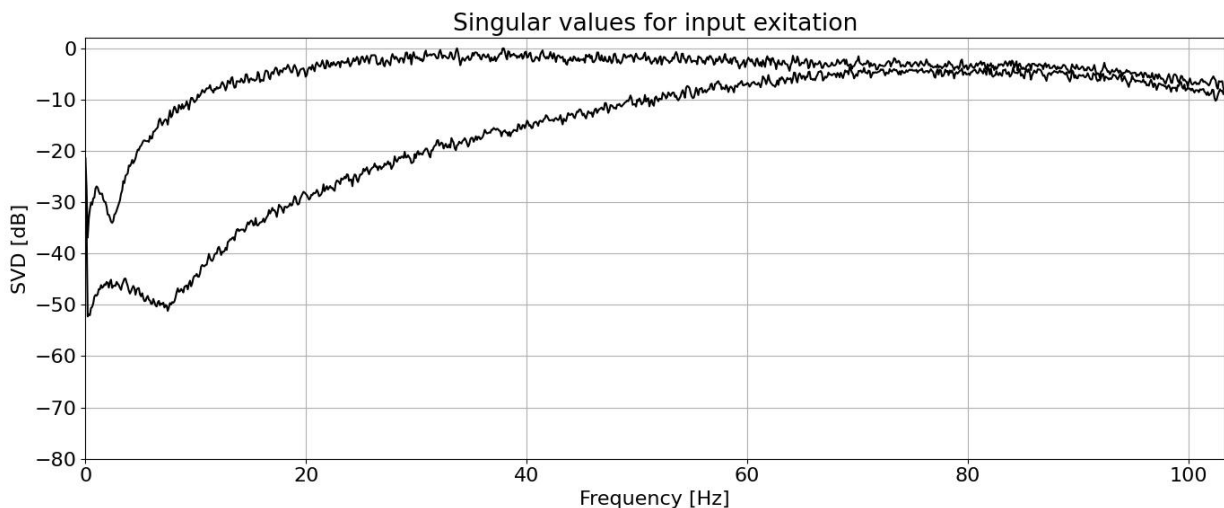


Figure 3: Shaker output force with Gaussian white noise and inverse filter noise input signals, respectively

The inverse filter noise shaker input was create by passing white noise through a digital filter with a magnitude squared response of $1/\text{frequency}$ in the frequency range 0.1 to 60 Hz, and flat above 60 Hz.

2.3 Tests

A total of 164 experimental modal tests were conducted in the test campaign, 32 tests with manual excitation, (35 in total where 3 were skipped due to sensor hits), and 4 x 33 tests with shaker excitation. The signals from the sensor were sampled at 1652 Hz and the total time series length of each test was 4 minutes, resulting in 397000 samples per test.

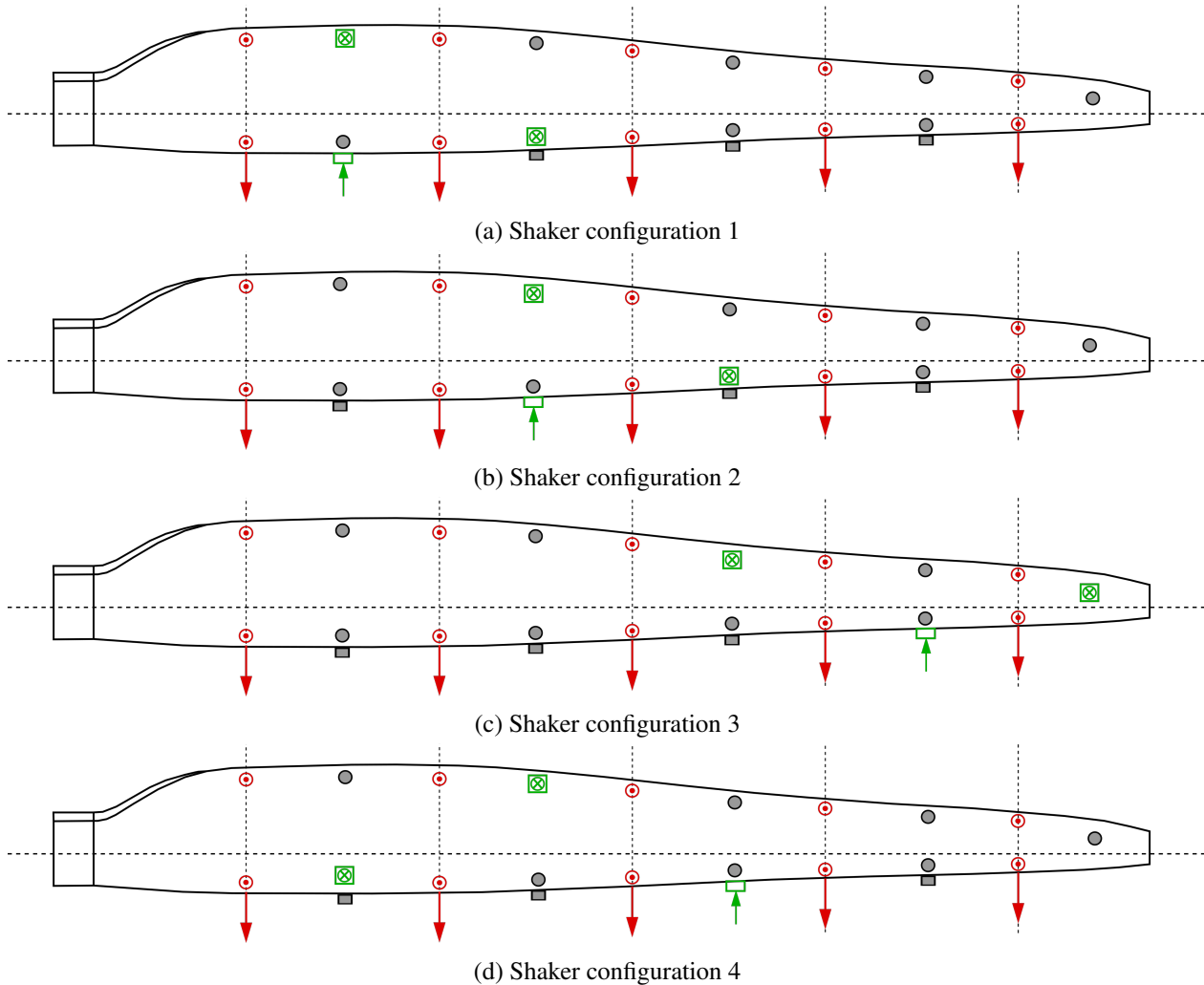


Figure 4: Shaker configuration 1 to 4. Shakers: , Masses:

2.4 Data analysis

System identification was done using Condensation of the correlation function [5] followed by the Time Domain Poly Reference (TDPR) [2] algorithm for identification. The correlation function was estimated using Welch averaging with 50% segment overlap [6]. The implementation used is part of the Manobiak Cloud OMA platform [7]. Singular value plots for this article were generated using Python [8] and Matplotlib [9].

2.4.1 Clustering

First identification was done on all data sets for a single configuration. This gave 33 repeated estimates for all poles. A particular pole was chosen and the 33 estimates for this pole were selected. The selection was

done by picking one of the frequencies and finding the 33 nearest neighbours. To make sure outliers were not included, the centroid of the group was selected. Using this as a new frequency the 33 nearest neighbours were reiterated. This procedure was repeated until no change to the centroid was seen. This is the same iteration as in the k-means clustering [10]. Note that for configurations 1 to 4 33 poles were found, but only 32 for the Manual configuration.

2.4.2 Filter bands

All data were downsampled to $f_s = 206.5 \text{ Hz}$, giving a Nyquist frequency of 103.25 Hz . In table 1 the filter bands used for the condensation algorithm are shown. Each filter had a pass band from f_1 to f_2 , and a guard band of $B_g = 1.24 \text{ Hz}$. Each condensation reduces the 15-channel correlation matrix function to $npoles$ and nid poles were chosen as physical from the band. The bands were from two different pipelines in the processing software [7].

Table 1: Filter bands used for the Condensation algorithm. (*) no stable pole was identified in this band.

band #	f_1 [Hz]	f_2 [Hz]	B_g [Hz]	$npoles$	nid	Pipeline
1	2.61	31.35	1.24	8	3	1
2	7.11	15.83	1.24	7	1	2
3	31.43	44.00	1.24	2	0*	1
4	44.00	65.53	1.24	3	2	1
5	65.40	87.71	1.24	3	2	1

3 Results

During this experiment, we generated an SVD plot for more than 30 experiments for each of the 4 configurations and the reference, i.e. more than 150 plots. A descriptive example for configuration 1 is shown in figure 5. This gives a first impression of the location of the modes of the structure.

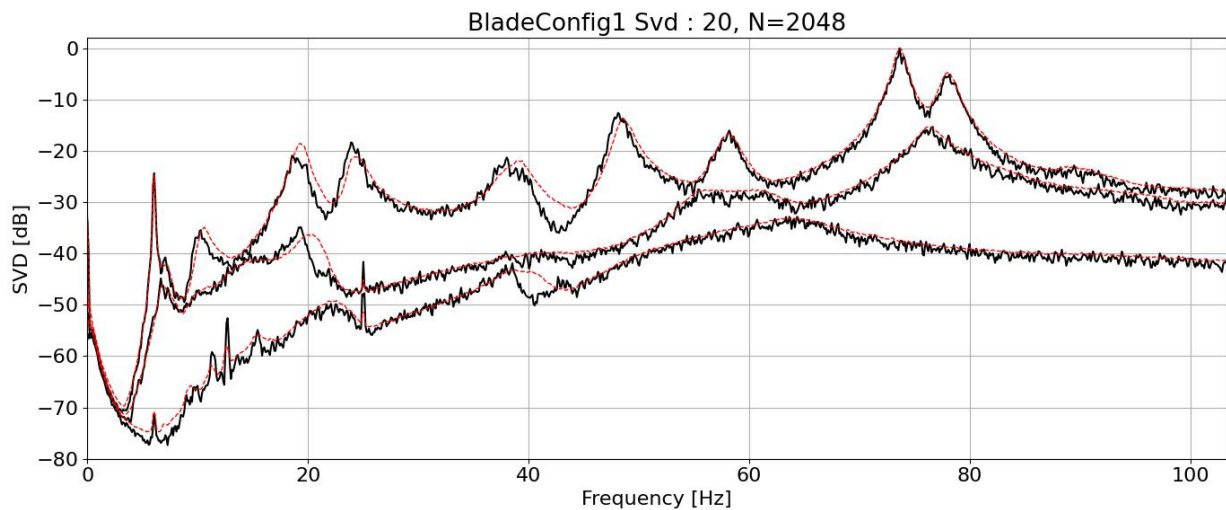


Figure 5: Overlay SVD plot of dataset 20 and the mean of all SVD plots (dashed line) of configuration 1.

The poles in the SVD plot in figure 5 correspond to the modes on the blade. A descriptive explanation of all modes is shown in table 2. The approximate frequency can be used to locate the corresponding peak in figure 5.

Table 2: Explanation of modes located at approximate frequency f_{approx} .

Mode	f_{approx} [Hz]	Description
1	6	1st bending, flap
2	11	1st bending, edge
3	19	2nd bending, flap, tip-brake in phase
4	24	2nd bending, flap, tip-brake out of phase
5	39	3rd bending, flap, tip-brake in phase
6	48	3rd bending, flap, tip-brake out of phase
7	58	2nd bending, edge
8	73	1st torsion, tip-brake in phase
9	78	1st torsion, tip-brake out of phase

3.1 Identified poles

The identified poles for all configurations are shown in tables 3 and 4. The standard deviation σ is shown next to all frequencies to ensure that no data are presented without a measure of uncertainty. Due to a large number of data sets in each configuration, we assume that the mean frequency is sampled from a normal distribution [11]. This means for the Manual excitation case any frequency estimate will be in the interval $[6.00 - 0.03, 6.00 + 0.03]$ with 68% probability, $[6.00 - 0.06, 6.00 + 0.06]$ with 95% probability, and $[6.00 - 0.09, 6.00 + 0.09]$ with 99.7% probability.

When an experiment has uncertainty there is no significant information in digits beyond the limit of uncertainty. Based on the size of the errors in this experiment, we present results with at most 4 significant digits as explained in [12]. For the frequencies above 10 Hz, 3 significant digits would be sufficient.

Table 3: Natural frequencies and standard deviations, mode 1 to 4

	Mode 1		Mode 2		Mode 3		Mode 4	
	f_{avg} [Hz]	σ [Hz]	f_{avg} [Hz]	σ [Hz]	f_{avg} [Hz]	σ [Hz]	f_{avg} [Hz]	σ [Hz]
Manual	6.00	0.03	10.46	0.21	19.31	0.13	24.13	0.23
Config. 1	6.05	0.01	10.57	0.29	19.52	0.26	24.25	0.33
Config. 2	6.06	0.01	10.47	0.22	19.21	0.24	24.19	0.30
Config. 3	6.16	0.06	10.41	0.20	19.27	0.28	24.30	0.25
Config. 4	6.05	0.01	10.47	0.20	19.45	0.20	24.13	0.34

Table 4: Natural frequencies and standard deviations, mode 5 to 8

	Mode 5		Mode 6		Mode 7		Mode 8	
	f_{avg} [Hz]	σ [Hz]	f_{avg} [Hz]	σ [Hz]	f_{avg} [Hz]	σ [Hz]	f_{avg} [Hz]	σ [Hz]
Manual	48.85	0.46	57.97	0.10	-	-	-	-
Config. 1	48.70	0.32	58.14	0.06	73.57	0.07	78.07	0.05
Config. 2	49.51	0.30	58.21	0.10	74.74	0.12	78.58	0.04
Config. 3	49.11	0.21	58.79	0.11	-	-	-	-
Config. 4	48.59	0.32	58.11	0.08	-	-	-	-

3.2 Average SVD plots

From tables 3 and 4 all frequencies are known. These results are shown in the average singular value plots for all configurations in figure 6, 7, 8, 9, and 10. Note that the apparent pole just below 40 Hz is not identified for any configuration.

This is because the experiment gave very poor stability of the SVD for this particular pole. At the very end of the experimental campaign, we learned that it was due to the loose cables hanging from the shakers, see figure 1. After fixing the shaker cables firmly to the blade, this pole could be identified as well.

Note that configurations 1 and 2 are the only configurations that have reliable identification of the two torsion modes above 70 Hz. Also, configuration 3 (figure 8) appears to put significantly less energy in all modes. We expect that this is explained by this shaker configuration having all excitation close to the softer tip of the blade.

From figure 10 it is apparent that the Manual excitation method is not able to excite the two torsion modes above 70 Hz. This points attention to the potential difficulty of manually exciting the torsion modes. This problem is also apparent from table 4. Configuration 1 and 2 show a significant difference in modes 7 and 8, above what can be explained by uncertainty. The estimated frequency of modes 7 and 8 differ by about 10 standard deviations in configurations 1 and 2 (for the largest standard deviation!). For all other configurations modes 7 and 8 are not identified.

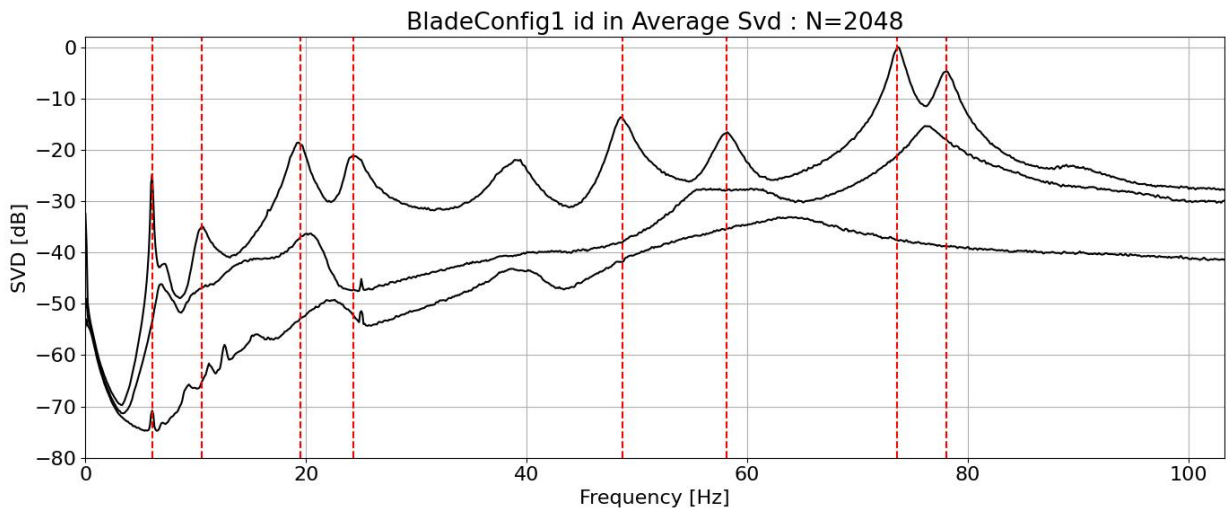


Figure 6: Mean SVD plot of BladeConfig1. Note: sufficient excitation of all modes.

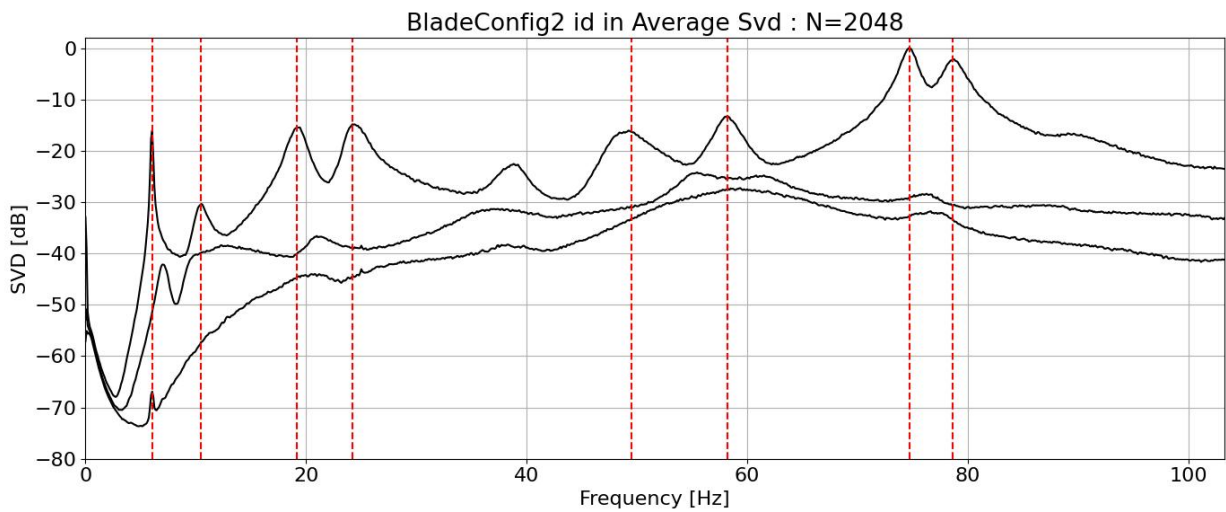


Figure 7: Mean SVD plot of BladeConfig2. Note: sufficient excitation of all modes.

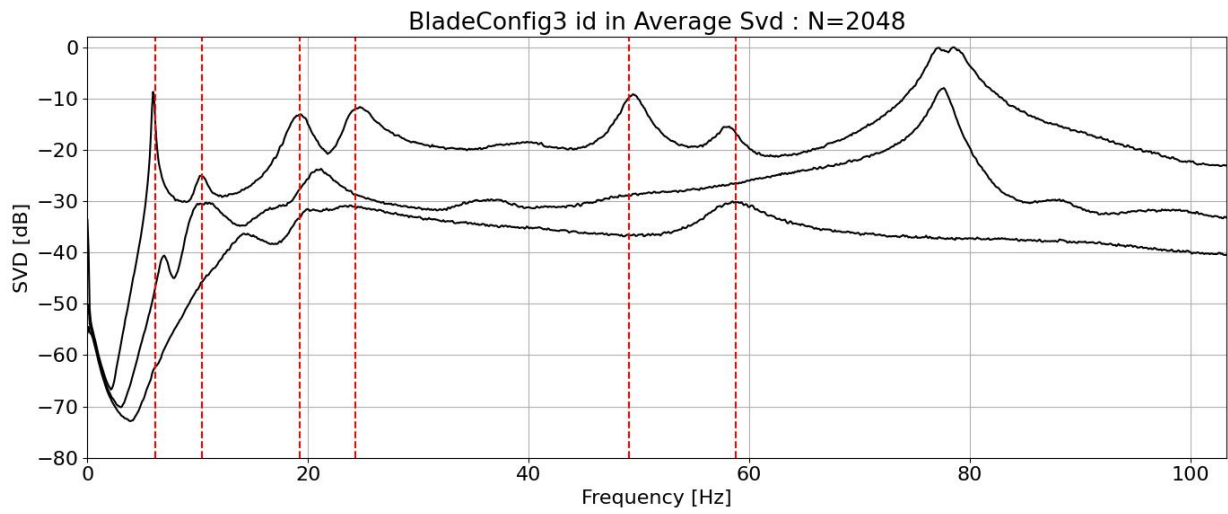


Figure 8: Mean SVD plot of BladeConfig3. Note: poor excitation of the torsion modes above 70 Hz, and almost no excitation of the in phase 3rd flap bending mode (see table 2).

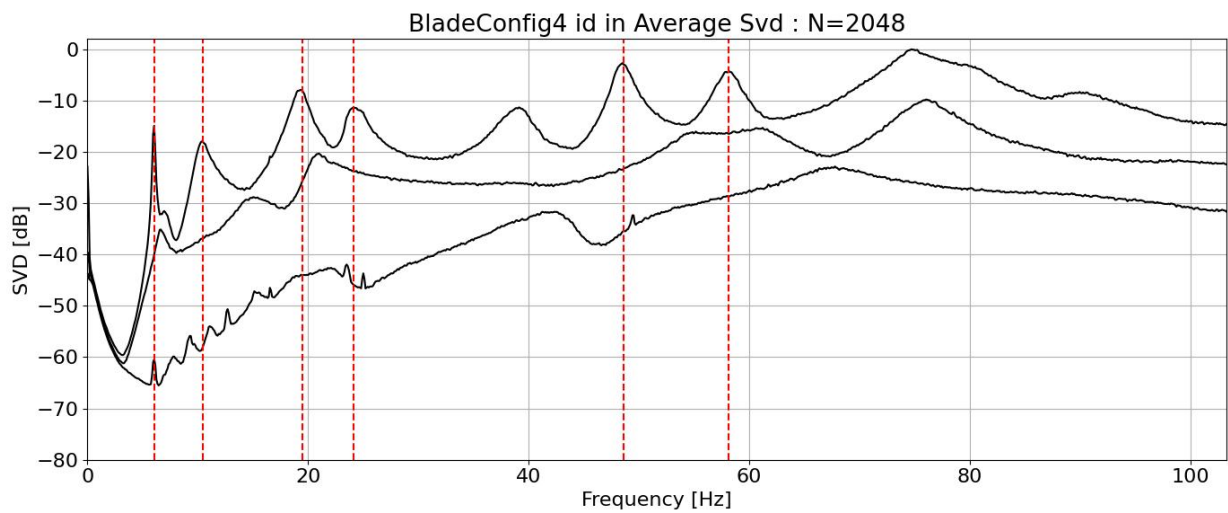


Figure 9: Mean SVD plot of BladeConfig4. Note: poor excitation of the torsion modes above 70 Hz.

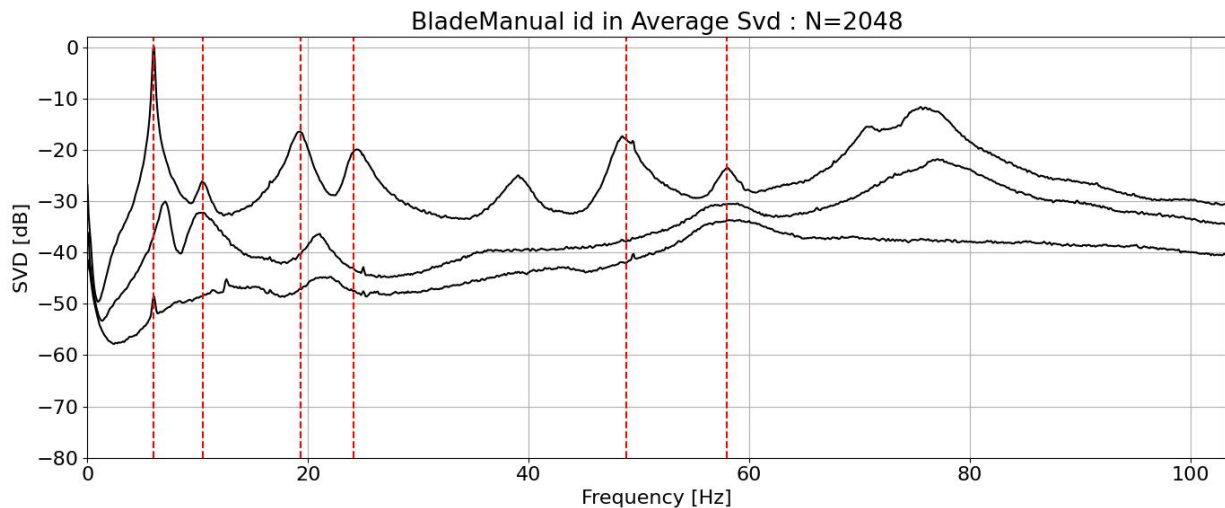


Figure 10: Mean SVD plot of BladeManual. Note: poor excitation of the torsion modes above 70 Hz.

4 Conclusion

Shaker configuration 1 and 2 gives similar results and they both exhibit good and consistent excitation of all modes. These are the best configurations, and they are geometrically very similar. For mode 7 and 8 further investigation is required to explain the significant difference in frequency estimates. Shaker configuration 3 fails to excite the in phase 3rd flap bending mode. In general, in this configuration, all modes are poorly excited. The torsion modes cannot be identified reliably. Shaker configuration 4 and the manual test have excited mode 1 to 6 well, but both fail to excite the two torsion modes. We have seen indications that configuration 4 will improve significantly with better cable fixing. For the manual tests, it may be more difficult to improve the excitation of the torsion modes.

We conclude that a set of 3 shakers can sufficiently excite a wind turbine blade so that all modes can be identified consistently and with very little variation. If the mass loading aspect of the approach can be dealt with, this approach will make OMA on blades more reliable and repeatable. Furthermore, this approach will eliminate the possibility of sensor hits and other human-induced impracticalities.

References

- [1] D. J. Ewins, *Modal testing: theory, practice and application*. John Wiley & Sons, 2009.
- [2] R. Brincker and C. Ventura, *Introduction to operational modal analysis*. John Wiley & Sons, 2015.
- [3] C. Rainieri and G. Fabbrocino, "Operational modal analysis of civil engineering structures," *Springer, New York*, vol. 142, p. 143, 2014.
- [4] "Olsen Wings A/S," <https://olsenwings.dk/>.
- [5] P. Olsen, M. Juul, and R. Brincker, "Condensation of the correlation functions in modal testing," *Mechanical Systems and Signal Processing*, vol. 118, pp. 377–387, Mar. 2019.
- [6] A. Brandt, *Noise and Vibration Analysis: Signal Analysis and Experimental Procedures*, ser. EBL-Schweitzer. Wiley, 2011.
- [7] "Manobiak ApS cloud oma platform," <https://manobiak.com/>, version 2022-06-25.

-
- [8] “Python,” <https://www.python.org/>, version 3.9.9.
- [9] “Matplotlib,” <https://matplotlib.org/>.
- [10] G. James, D. Witten, T. Hastie, and R. Tibshirani, *An introduction to statistical learning*. Springer, 2013.
- [11] R. Johnson and I. Miller, *Miller & Freund’s Probability and Statistics for Engineers*. Pearson Prentice Hall, 2005.
- [12] N. C. Barford, *Experimental measurements*, 2nd ed. Chichester, England: John Wiley & Sons, Oct. 1985.